Journal of Cellular Biochemistry 89:576–588 (2003)

hMad4, c-Myc Endogenous Inhibitor, Induces a Replicative Senescence-Like State When Overexpressed in Human Fibroblasts

Richard Marcotte,[1] Jing-Fang Qian,[2] James Chen,[1] and Eugenia Wang[2]*

[1]The Bloomfield Center for Research in Aging, Lady Davis Institute for Medical Research, The Sir Mortimer B. Davis-Jewish General Hospital and Department of Medicine, McGill University, Montréal, Québec, Canada
[2]Department of Biochemistry and Molecular Biology, University of Louisville School of Medicine, Louisville, Kentucky

Abstract Mad family proteins have an antagonistic action on Myc-dependent cell proliferation and transformation. We isolated a human cDNA clone, human Mad4 (hMad4), encoding a polypeptide of 209 amino acid residues, exhibiting 90% identity with mouse Mad4. Northern blot analysis shows that hMad4 probe hybridizes to a 3.8 kb message; its expression is highest in quiescent human WI38 fibroblasts. Among tissues, hMad4 mRNA is most abundant in brain, lung, and muscle. Consistent with other members of the Mad family, hMad4 can repress the transactivation activity of Myc/Max heterodimers on an E-box chloramphenicol acteyl transferase (CAT) reporter plasmid; inhibition of both proliferation and clonogenic formation of hMad4-infected cells correlates with the in vitro reporter repression. Moreover, infection of young human fibroblasts induces a replicative senescence-like state. This phenotype was accompanied by s-β-galactosidase and PAI-1 expression. These results suggest that hMad4 might be an important regulator of replicative senescence in human cells. J. Cell. Biochem. 89: 576–588, 2003.

Key words: senescence; hMad4; c-Myc

The c-Myc proto-oncogene encodes a nuclear phosphoprotein that functions as a transcription factor, regulating gene expressions important for cell proliferation and differentiation [Dang, 1999]. Overexpression of c-Myc in cultured cells can inhibit differentiation, induce neoplastic transformation, and initiate apoptosis [Facchini and Penn, 1998; Prendergast, 1999]. Gene amplification, insertional mutagenesis, and chromosomal translocations are frequently found in naturally occurring tumors at the Myc loci [Nesbit et al., 1999]. Like most regulatory transcription factors, c-Myc encodes two separable domains, a C-terminal DNA binding domain containing the basic helix-loop-helix/leucine zipper (bHLH/LZ) [Kato et al., 1990], and an N-terminal transactivation domain [Blackwell et al., 1990]. c-Myc protein heterodimerizes with Max, through the basic region of the bHLH/LZ domain [Blackwood and Eisenman, 1991; Amati et al., 1993a,b]. This Myc–Max dimer binds to a core consensus DNA sequence, CA(C/T)GTG, referred to as the Myc E-box [Blackwell et al., 1990; Kato et al., 1990]. This sequence is found in a variety of genes involved in cell cycle progression and apoptosis, regulated by c-Myc [Dang, 1999]; recent microarray experiments suggest a role for c-Myc in metabolism, cell growth, and adhesion [Coller et al., 2000; Guo et al., 2000; Nesbit et al., 2000; O'Hagan et al., 2000; Schuhmacher et al., 2001].

In general, Max expression is very stable, and constant in all cellular stages, including the transition from quiescence to replication [Berberich et al., 1992; Blackwood et al., 1992], while the regulation of c-Myc expression is

Grant sponsor: National Institute on Aging, National Institutes of Health, USA (to E.W.); Grant number: R01 (AG09278).

*Correspondence to: Dr. Eugenia Wang, Department of Biochemistry and Molecular Biology, University of Louisville School of Medicine, Louisville, Kentucky 40292.
E-mail: Eugenia.Wang@Louisville.edu

Received 13 December 2002; Accepted 5 February 2003
DOI 10.1002/jcb.10517

variable [Hann et al., 1985; Rabbitts et al., 1985] and rapidly modulated during cell cycle entry and exit [Luscher and Eisenman, 1990]. This constant versus variable expression between *Max* and *Myc* gene expression has prompted the search for other Max-associated proteins, leading to the identification of other partners for Max, such as human Mad1 [Ayer et al., 1993], human Mxi1 [Zervos et al., 1993], mouse Mad3, and mouse Mad4 [Hurlin et al., 1995] (referred to as Mad family members). These proteins specifically interact with Max, forming heterodimeric complexes that bind to the same Myc E-box sequence.

In contrast to Myc–Max heterodimers, which activate transcription, Mad dimers negatively regulate transcription [Ayer et al., 1993; Zervos et al., 1993; Hurlin et al., 1995] by binding to mSin3, a mammalian homologue of a yeast transcriptional repressor [Ayer et al., 1995; Schreiber-Agus et al., 1995]. The Mad/Max/mSin3 complex associates with histone deacetylases HDAC1 and HDAC2 [Hassig et al., 1997; Laherty et al., 1997], which fold chromatin into a state inaccessible to transcriptional activation. Therefore, overexpression of known Mad proteins inhibits cell cycle progression [Chen et al., 1995], and suppresses Myc-dependent transformation [Lahoz et al., 1994; Hurlin et al., 1995; Koskinen et al., 1995].

During the transition from proliferation to differentiation, a switch in expression between Myc and Mad has also been found, possibly to ensure non-proliferating status in terminally differentiated cells [Ayer and Eisenman, 1993; Hurlin et al., 1995; Cultraro et al., 1997]. Consistent with a role in differentiation and cell proliferation, mice lacking Mad1 are defective in granulocyte differentiation [Foley et al., 1998]. Surprisingly, these mice do not show any other apparent differentiation defect, possibly because of functional redundancy among other Mad family members [Foley et al., 1998]. This redundancy does not necessarily extend to all Mad family members, since mice defective for Mxi1 exhibit defects in maintenance of mature organs, cellular growth, and cancer suppression [Schreiber-Agus et al., 1998]. On the other hand, homozygous deletion of mouse Mad3 had no obvious defect in development or differentiation but cells from these mice were more sensitive to radiation-induced apoptosis [Queva et al., 2001]. So far, no Mad4 knock-out mice have been described.

We report here the isolation and characterization of a human member of the Mad family that shows a strong structural homology of 90% with mouse Mad4, and thus is referred to here as human Mad4 (hMad4). Functionally, hMad4 behave exactly like mouse Mad4 by dimerizing with Max as well as repressing the expression of a reporter gene under a synthetic E-box promoter. Moreover, hMad4 repressed cell proliferation and clonogenic expansion of transformed cells. Overexpression in normal human fibroblasts induced a phenotype reminiscent of replicative senescence. The present results suggest that hMad4 regulates both cell proliferation and replicative senescence by acting as a transcriptional repressor.

MATERIALS AND METHODS

GenBank Accession Number for hMad4 Nucleotide Sequence: AF082740

Isolation of cDNA clone. Clones (6×10^5) of a lambda Zap expression library containing 80% senescent human fibroblast cDNA with the remaining 20% from confluent quiescent state (this library was the generous gift of Dr. Judith Campisi) were induced with 10 mM isopropyl-1-thio-*b*-D-galactopyranoside (IPTG), and used to isolate several positive phage clones with an antibody specific to non-proliferating cells, originally produced by injecting the cytoskeletal fraction of senescent fibroblasts in mice [Wang, 1985a,b]. pBK-CMV phagemids containing the insert were excised from the lambda ZAP expression vector using ExAssist interference-resistant helper phage (Stratagene, LaJolla, CA). In order to isolate additional clones containing full-length transcript, one million phages from a human hippocampus cDNA library (Stratagene) were screened using a 600 bp ^{32}P-labeled SacI-SacI fragment of one of the original clones, ST931, according to the manufacturer's recommendation. Selected positive clone inserts were subcloned into pBluescript SK (−) (Stratagene) and processed for DNA sequencing on an Applied Biosystems model 310 automated sequencer, using a dye terminator cycle sequencing kit (Perkin-Elmer, Mississauga, ON). Both strands were sequenced using vector-cDNA-specific primers. Nucleotides and deduced protein sequences were analyzed using the PC/GENE software package (IntelliGenetics, Inc., Campbell, CA) and the National Center for Biotechnology Information BLAST program.

Northern blot analysis. Total RNA was isolated from WI38 normal human fibroblasts, and different human tissues, using Trizol reagent following the manufacturer's recommendation. Human tissues were obtained from autopsy specimens of a 68-year-old individual. Cell lines were maintained in culture according to the previously described method [Wang, 1985b]. Ten micrograms of total RNA were fractionated on a 1% agarose gel and blotted onto a nylon membrane; blots were hybridized with the ^{32}P-labeled cDNA SacI fragment, and hybridization was performed overnight at 42°C in a solution of 50% formamide, 10 × Denhardt's solution, 0.1% sodium pyrophosphate, 50 mM Tris pH 7.5, 10% dextran sulfate, 1% sodium dodecyl sulfate (SDS), and 100 μg/ml of denatured salmon sperm DNA (Roche, Laval, QC). Membranes were washed once at room temperature in 2 × sodium chloride/sodium citrate (SSC) buffer containing 1% SDS for 30 min, and three times at 65°C for 15 min. Membranes were then exposed to X-ray films at −70°C with intensifier screens. The same membranes were stripped and reprobed with human 18S ribosomal RNA probe to verify the amount of total RNA loaded in each lane.

CAT assay. A chloramphenicol acetyl transferase (CAT) reporter vector was constructed by inserting a *CAT* gene in the multiple cloning site of the pBK-CMV vector. The E-box sequence from the ornithine decarboxylase (ODC) promoter [Bello-Fernandez et al., 1993], 5′TGC GGC **CAC GTG** TCG CGA3′, was inserted three times in the Sac site 5′ of the *CAT* gene. c-Myc and Max cDNAs were amplified from a HeLa cDNA library by PCR with the following primers: c-Myc; 5′TGCCTCCCGCTTTGTGTG3′ and 5′GTTGTGAGGTTGCATTTGA3′; Max; 5′CGGGAAATGAGCGATAACGA3′ and 5′CGTTTTATTGCTGGCCTGCC3′. PCR fragments were subcloned, confirmed by sequencing, and then subcloned into AP2 (a generous gift of Dr. Jacques Galipeau [Galipeau et al., 1999]) to give rise to AP2-CMV-Max, AP2-CMV-c-Myc, AP2-CMV-hMad4, hMad4L-P16, and empty-vector. Human embryonic kidney 293 cells were transfected using the calcium phosphate procedure, collected 48 h later, lysed by freezing and thawing cycles, and centrifuged to remove cellular debris. Cellular extracts were incubated overnight with ^{3}H-chloramphenicol and butyryl-CoA as a donor. Butyrylated ^{3}H-chloramphenicol was extracted with several rounds of organic extraction and counted with a scintillation counter.

Co-immunoprecipitations and Western blots. Human embryonic kidney 293 cells were transfected using Lipofectamine reagent, following the manufacturer's recommendations (Canadian Life Technologies, Inc., Burlington, ON). Cells were lysed in ice-cold lysis buffer (1X PBS, 1% Nonidet P-40, 10 mM NaF, 1 mM Na_3VO_4, 1 mM PMSF, 1 μg/ml aprotinin, 1 μg/ml pepstatin, and 0.5 μg/ml leupeptin), sonicated, and centrifuged briefly to remove genomic DNA. The supernatant was removed and immunoprecipitated at 4°C with the indicated antibodies; anti-Myc (14851A) and anti-Max (65741A) were purchased from Pharmingen (Mississauga, ON), and anti-hMad4 was produced in our laboratory by injecting the peptide corresponding to amino acids 189–209 of the hMad4 C-terminus into a rabbit. Protein-G agarose beads (Sigma, Oakville, ON) were then added to the mixture for 3 h under constant rotation. Immunoprecipitates were washed three times with ice-cold PBS, resuspended in SDS–polyacrylamide gel (PAGE) loading buffer, heated at 95°C for 10 min, and centrifuged briefly to remove agarose beads. Supernatants were resolved on 12% SDS–PAGE and processed following standard immunoblotting procedure.

In the case of Western blot from cell lysates, proteins were extracted by scraping cells in buffer F [Sommer et al., 1998], left on ice for 30 min, and then spun down 2 min at maximum speed to remove cellular debris. Proteins were quantified using BioRad protein assay following the manufacturer's recommendations. Fifty micrograms of total proteins were loaded and separated on 15% acrylamide gels, transferred on nitrocellulose membranes, blocked 1 h at room temperature, and incubated overnight at 4°C with the following antibodies: PAI-1 (Santa Cruz no. sc-8979), b-actin (Santa Cruz no. sc-8432).

Retroviral infection, proliferation assay, and colony assay. HeLa and 293 cells were infected with a bi-cistronic retroviruses coding for hMad4 and EGFP protein. Briefly, the vectors described above were co-transfected using Lipofectamine in a packaging cell line, along with a vector carrying a bleomycin selection marker. Transfected cells were selected for 3–4 weeks and then processed by fluorescent-activated cell sorting (FACS). Supernatants from green producers were used to infect target

cells, which were sorted, plated, and amplified for subsequent experiments. In the case of proliferation assays, equal numbers of sorted empty-vector- and hMad4-infected cells were plated in triplicate. Cells were harvested and counted every day for 4 days with a hematocytometer. In the case of colony assays, equal numbers of sorted infected cells were mixed in 0.3% agar and plated on 0.6% agar. Cells were fed every 4 days with Dulbecco's modified Eagle's medium (DMEM) supplemented with 10% fetal bovine serum (FBS). After 2 weeks, colonies were visible macroscopically; total number of colonies on each plate were counted. The experiment was done in triplicate.

Replicative senescence and s-β-galactosidase staining. WI38 cells were passaged until the doubling time was more than 3 weeks at which point cells were considered senescent. s-β-galactosidase staining was done as described in Serrano et al. [1997].

RESULTS

Isolation of an hMad4 cDNA Clone

Several clones, upregulated in senescent cells, were isolated from a normal human fibroblast library using a non-proliferating cell specific antibody. Partial sequencing and computer search revealed that one of the clones, ST931, which was 2 kb in length, did not match any known cDNA sequence. Since a poly(A) signal was not detected in the ST931 sequence, a human hippocampus cDNA library was screened with a 677 bp Sac1 probe from ST931 in an attempt to isolate a full-length cDNA; twenty positive clones were isolated. One clone, hl8-3, containing the longest insert (about 3.2 kb), was selected for further analysis by sequencing. Sequencing showed that hl8-3 contains a poly(A) tail and a 1.4 kb overlapping sequence with ST931. Aligning the hl8-3 and ST931 clone sequences established nucleotide information for the putative full-length cDNA sequence, which is putatively 3.8 kb in length (Fig. 1A). A single open reading frame appears in this cDNA sequence; the start codon is consistent with Kozak's consensus sequence [Kozak, 1987]. The coding region predicts a 209 amino acid protein, a predicted molecular mass of 23.5 kDa, and an estimated pI value of 6.5.

Computer search on the GenBank protein sequence data banks showed that the deduced amino acid sequence has 90% identity with the mouse *Mad4* gene (Fig. 1B). Divergence is higher at the C-terminal end between the human and murine clones, explaining why the original sequence of probe ST931, which spans the C-terminus, showed no homology to any known gene. This result indicates that this clone is likely to be the human homologue of mouse Mad4, and is referred to henceforth as human Mad4 (hMad4). Two other members of the human Mad family (Mad1 and Mxi1) have been previously characterized [Ayer et al., 1993; Zervos et al., 1993]. An alignment of the amino acid sequence of hMad4 with human Mad and Mxi1 revealed 48% identity with human Mad1, and 52% identity with human Mxi1 (Fig. 1B). Members of the Mad family contain two highly conserved regions: the bHLHZip domain and an N-terminal region encompassing the mSin3-interacting domain (SID), which is responsible for transcriptional repression. These two regions are also found in hMad4, and are highly homologous; however its extreme C-terminus is very different from those reported for both human Mad and Mxi1 (Fig. 1B).

GenBank analysis revealed that our full-length hMad4 cDNA nucleotide sequence is distributed between two cosmid sequences, HW2 and L33c6, known to contain part of the Huntington's disease candidate region [Baxendale et al., 1993]. Further sequence analysis allowed us to determine that the *hMad4* gene consists of six exons, which are all coding for the actual protein and are indicated in Figure 1A and five introns, and spans about 15 kb. Since cosmids L33c6 (GenBank Z68282) and HW2 (GenBank Z49250) contain the full-length clone of hMad4 cDNA, the position of hMad4 can thus be assigned to chromosome 4p16.3.

Expression of hMad4 in Tissues and Cell Lines

A 677 bp SacI fragment from the 3′untranslated region was used in Northern blot analysis to determine the expression of hMad4 in tissues and cell lines. When Northern blot analysis was performed on RNA isolated from several human tissues, a single transcript of 3.8 kb was found to be present in brain, lung, heart, kidney, liver, and muscle, while an additional 1.6 kb band is found in muscle and possibly in kidney and lung (Fig. 2A). Other Mad members are induced in growth-arrested cells. To test whether hMad4 is also upregulated in growth-arrested states, total RNA extracted

A

```
                                                    +1
ccgtcccggggcggacgggcgcgggcgggaggATG GAG CTG AAC TCC CTG CTG ATC CTG CTG GAG GCG GCC GAG   42
                                  Met Glu Leu Asn Ser Leu Leu Ile Leu Leu Glu Ala Ala Glu   14
            I                  ↓
TAC CTG GAG CGC AGG GAT CGA GAG GCC GAG CAC GGC TAC GCC TCG GTG CTG CCC TTC GAC GGC GAC  108
Tyr Leu GLu Arg Arg Asp Arg Glu Ala Glu His Gly Tyr Ala Ser Val Leu Pro Phe Asp Gly Asp   36
                                        II                        ↓
TTC GCC AGG GAG AAA ACA AAG GCG GCC GGC CTG GTG CGC AAG GCC CCG AAC AAC AGG TCT TCA CAC  174
Phe Ala Arg Glu Lys Thr Lys Ala Ala Gly Leu Val Arg Lys Ala Pro Asn Asn Arg Ser Ser His   58
          III              ↓
AAC GAG CTA GAA AAG CAC AGA CGA GCC AAA CTC AGG CTG TAC CTT GAG CAG CTC AAG CAA CTG GTG  240
Asn Glu Leu Glu Lys His Arg Arg Ala Lys Leu Arg Leu Tyr Leu Glu Gln Leu Lys Gln Leu Val   80
                                     IV
CCC CTG GGC CCC GAC AGC ACC CGC CAC ACC ACG CTG AGC CTC CTG AAG CGG GCC AAG GTG CAC ATC  306
Pro Leu Gly Pro Asp Ser Thr Arg His Thr Thr Leu Ser Leu Leu Lys Arg Ala Lys Val His Ile  102
 ↓
AAG AAA CTG GAG GAG CAG GAC CGC CGG GCA CTG AGC ATC AAG GAG CAG CTG CAG CAG GAG CAT CGT  372
Lys Lys Leu Glu Glu Gln Asp Arg Arg Ala Leu Ser Ile Lys Glu Gln Leu Gln Gln Glu His Arg  124
                        V
TTC CTG AAG CGG CGC CTG GAG CAG CTG TCG GTG CAG AGC GTG GAG CGC GTG CGC ACA GAT AGC ACG  438
Phe Leu Lys Arg Arg Leu Glu Gln Leu Ser Val Gln Ser Val Glu Arg Val Arg Thr Asp Ser Thr  146
                                    ↓
GGC TCT GCT GTC TCC ACG GAC GAC TCA GAG CAA GAA GTG GAC ATA GAG GGC ATG GAG TTT GGC CCT  504
Gly Ser Ala Val Ser Thr Asp Asp Ser Glu Gln Glu Val Asp Ile Glu Gly Met Glu Phe Gly Pro  168

GGT GAG CTG GAC AGT GTT GGC AGC AGC AGT GAC GCG GAC GAC CAC TAC AGC CTG CAG AGT GGC ACC  570
Gly Glu Leu Asp Ser Val Gly Ser Ser Ser Asp Ala Asp Asp His Tyr Ser Leu Gln Ser Gly Thr  190
                                     VI
GGC GGC GAC AGT GGC TTC GGG CCC CAC TGC CGG CGG CTG GGC CGC CCC GCC CTC TCG TAGgcccg….  638
Gly Gly Asp Ser Gly Phe Gly Pro His Cys Arg Arg Leu Gly Arg Pro Ala Leu Ser  *          209
```

B

```
                                SID
hMad4   MELNSLL---ILLEAAEYLERRERE AEHGYASVLPF----------DGDFARE   40
mMad4   MELNSLL---LLLEAAEYLERRERE AEHGYASXLPF----------DGDFARK   40
hMad1   MAAAVRMNTOMLLEAADYLERRERE AEHGYASMLPY--------NNKDRDALKRR  47
hMxi1   MERVKMINVQRLLEAAEFLERRERE CEHGYASSFPSMPSPRLQHSKPPRRLSRA  54
                                Basic Region      Helix 1      Loop
hMad4   KTKAAGLVRKAPNNRSSHNELEKHRRAKLRLYLEQLKQLVPLGPDSTRHTTLSL   94
mMad4   KTKTAGLVRKGPNNRSSHNELEKHRRAKLRLYLEQLKQLGPLGPDSTRHTTLSL   94
hMad1   NK----SKKNNSSSRSTHNEMEKNRRAHLRLCLEKLKGLVPLGPESSRHTTLSL  97
hMxi1   QKHSSGTSNTSTANRSTHNELEKNRRAHLRLCLERLKVLIPLGPDCTRHTTLGL  108
        Helix 2                 Leucine Zipper
hMad4   LKRAKVHIKKLEEQDRRALSIKEQLQQEHRFLKRRLEQL-SVQSVERVRTDSTG  147
mMad4   LKRAKXHIKKLEEQDRRALSIKEQLQREHRFLKRRLEQL-SVQSVERVRTDSTG  147
hMad1   LTKAKLHIKKLEDCDRKAVHQIDQLQREQRHLKRQLEKL----GIERIRMDSIG  147
hMxi1   LNKAKAHIKKLEEAERKSQHQLENLEREQRFLKWRLEQLQGPQEMERIRMDSIG  162

hMad4   SAVSTDDSEQ-----EVDIEGMEFGPGELDSVGSS--SDADDHYSLQSGTGGDS  194
mMad4   SAVSTDDSEQ-----EVDIEGMEFGPGELDSAGSS--SDADDHYSLQSSGCSDS  194
hMad1   STVSSERSDSDREEIDVDVESTDYLTGDLDW-SSSSVSDSDERGSMQS-LGSDE  199
hMxi1   STISSDRSDSEREEIEVDVESTEFSHGEVDNISTTSISDIDDHSSLPS-IGSDE  215

hMad4   GFGPHC-RRLG-----RPALS-                                   209
mMad4   SYGHPC-RRPG-----CPGLS-                                   209
hMad1   GYSSTSIKRIKLQDSHKACLGL                                   221
hMxi1   GYSSASVK---------LSFTS                                   228
```

Fig. 1. **A**: The nucleotide and deduced amino acid sequences of hMad4. The open reading frame is shown in uppercase letters, and 5′- and 3′-noncoding regions are shown in lowercase letters. The deduced amino acid residues are depicted below the open reading frame. The numbers at the right of each line refer to the nucleotide positions and amino acid positions, respectively. The nucleotide and amino acid sequences are numbered starting with the first ATG in the open reading frame (+1). The asterisk (*) indicates the translation termination codon. Arrows indicate exon–intron boundaries, and the six exons are numbered I–VI. **B**: Comparison of the amino acid sequence of hMad4 with murine Mad4 and of the other members of the human Mad family. The sequence alignments were generated using PC/GENE software. The shadowed regions indicate conserved amino acid residues. The SID and bHLHZip regions are overlined. The number of amino acid residues is shown at the right.

from different replicating and quiescent stages of fibroblast cultures at young and intermediate stages of the in vitro life span, as well as their senescent counterparts, were run for Northern blot analysis. The probe detected one single transcript of 3.8 kb (Fig. 2B). Results for young, intermediate, and senescent cells show that the mRNA level is very high in quiescent as well as senescent cells, but is relatively low in replicating cells, indicating that hMad4 expression is growth arrest-dependent (Fig. 2B). The level of 18S rRNA was used as loading control.

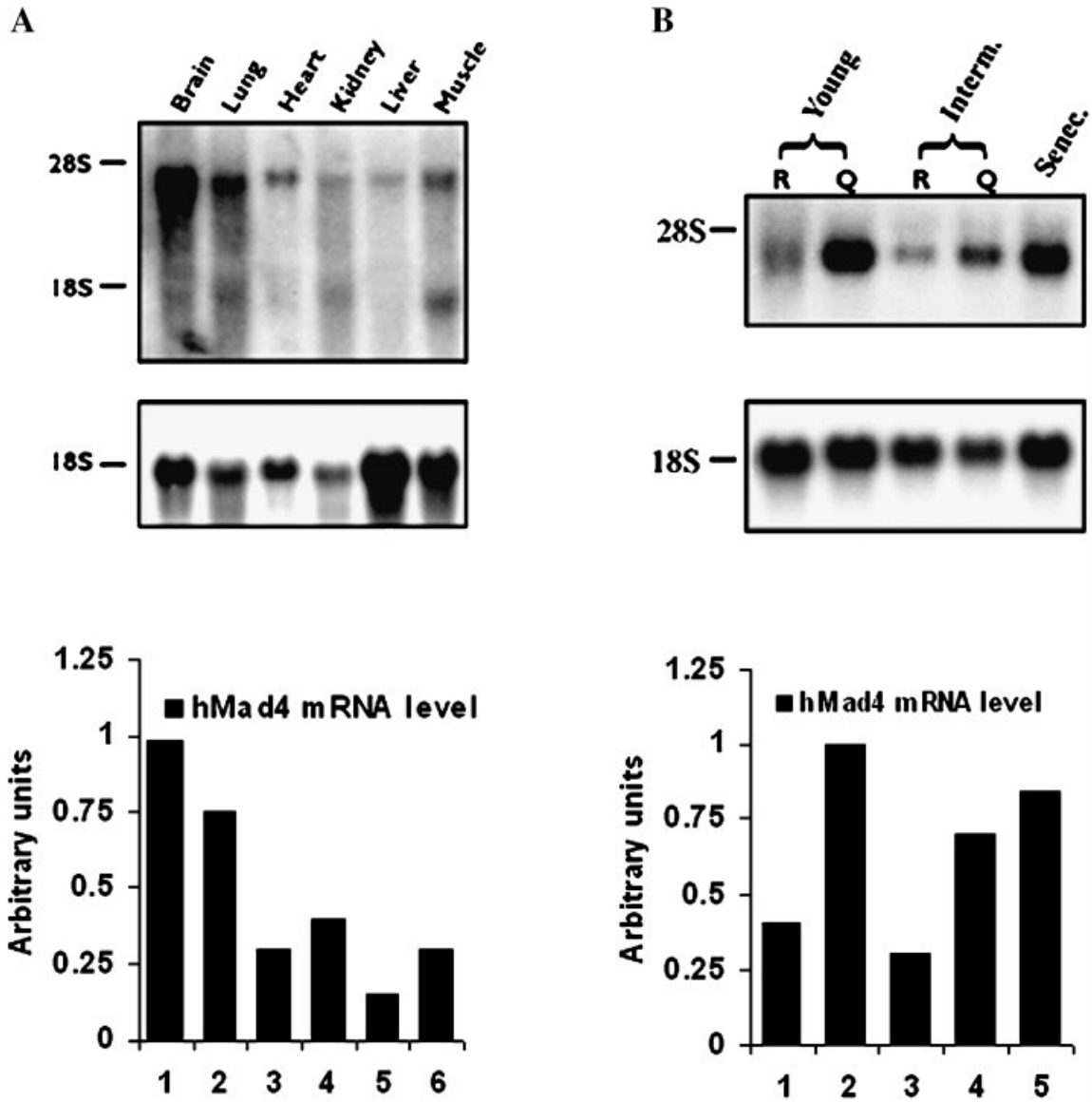

Fig. 2. Expression of hMad4 mRNA in tissues and cell lines. Blots were hybridized with the hMad4 probe as described under ''Materials and Methods.'' Blots were stripped and reprobed with an 18 S probe to control loading. Graphs are expressed as hMad4 level over 18S level, where the highest signal was given a value of 1. **A**: Expression of hMad4 in different human tissues. A major mRNA was detected at 3.8 kb, with a minor band of 1.6 kb found only in muscle and possibly kidney and lung. Each lane contains 10 μg of total RNA. Tissues used for analysis are denoted at the top. **B**: Expression of hMad4 mRNA in growth-arrested and replicating cells. Ten micrograms of total RNA was used for Northern blot analysis, as described under ''Materials and Methods.'' Replicating cells (R, 50% confluent); quiescent cells (Q, contact inhibited for at least 3 days); senescent cells (senec); young, WI38 normal human fibroblast cell line cultures at early stage of their in vitro life span [cumulative population doubling level (CPDL = 18)]; cultures at their intermediate stage of life span (interm, CPDL = 46). Senescent human fibroblasts were cultures at their final stage of replicating life span with CPDL = 58.

hMad4 Represses E-box-Mediated Gene Transcription

Since other Mad family members heterodimerize with Max to promote functional repression [Ayer et al., 1993; Zervos et al., 1993; Hurlin et al., 1995], co-immunoprecipitation was performed to determine whether hMad4 can associate with Max. Human embryonic kidney 293 cells were co-transfected with c-Myc- and Max-, hMad4- and Max- or c-Myc- and hMad4-AP2-derived vectors. After 48 h, transfected cells were subjected to low stringency immunoprecipitation with anti-Max and anti-hMad4. The immunoprecipitates were subjected to SDS–PAGE and analyzed by Western

blot, with anti-c-Myc, anti-Max, anti-hMad4, and secondary antibody alone (not shown). As a positive control, anti-Max was able to efficiently co-immunoprecipitate c-Myc in cells transfected with Max and c-Myc (lane 4 in the top panel in Fig. 3A). Furthermore, anti-Max and anti-hMad4 are able to co-immunoprecipitate hMad4 and Max, respectively (lanes 5 and 2 in Fig. 3A), while c-Myc is not immunoprecipitated by anti-hMad4 (lane 3). These results indicate that, like other Mad members, hMad4 associates with Max but not c-Myc, and likely requires this association to bind DNA.

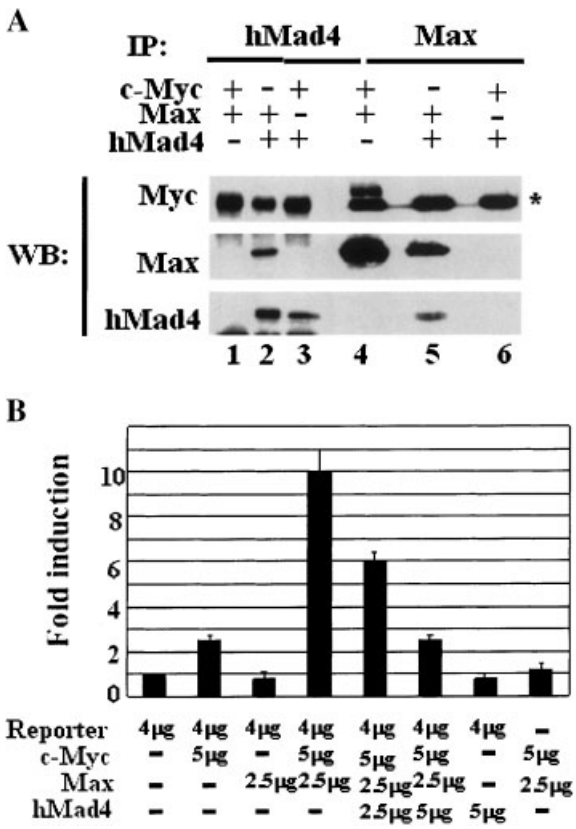

Fig. 3. **A**: Immunoprecipitation of c-Myc, Max, and hMad4—Immunoprecipitation was performed as described in ''Materials and Methods.'' **Lanes 1–3** are cell lysates from transfected 293 cells immunoprecipitated with anti-hMad4, while lanes **4–6** are immunoprecipitated with anti-Max. Western blots show, in order from **top** to **bottom**, c-Myc, Max, and hMad4, respectively after immunoblotting of the immunoprecipitates with the corresponding antibody. Asterisk (*) represents the IgG strong background signal. **B**: CAT assay—Along with the transfected product shown in Figure 5B, each transfected set of cells were transfected with a β-galactosidase expression vector to control transfection efficiency. Amount of total DNA was normalized to equal amounts by completing with empty AP2 vector. Last lane of the histogram, cells were transfected with a CAT reporter construct that does not contain any E-box binding site. CAT activity was measured as described in ''Materials and Methods.'' Each set of transfections was done in triplicate.

The association of hMad4 with Max strongly suggests that these dimers may bind DNA, specifically at E-box sequences, and thus repress transcription. Using a CAT reporter construct, in vivo transcriptional repression was examined. Again, 293 cells were co-transfected with a combination of c-Myc-, Max-, and hMad4-AP2-derived vectors, along with a CAT reporter construct (see Materials and Methods); 48 h later CAT activity was analyzed. When c-Myc and Max were co-transfected in 293 cells, there was a 10-fold increase in CAT activity over cells transfected with the reporter construct alone. When hMad4 was co-transfected with c-Myc and Max at increasing amount, there was a 4-fold decrease in CAT activity, similar to the activity seen with transfection of c-Myc alone (Fig. 3B). Transfection with c-Myc alone resulted in 2- to 3-fold increase in CAT activity, in concordance with other published reports [Ayer et al., 1993; Zervos et al., 1993; Hurlin et al., 1995], since Max is thought not to be the limiting factor in vivo for the formation of active dimers. Expression levels of transfectants were verified by western blots and found to be equal (data not shown). These results indicate that hMad4 represses c-Myc transcriptional activity, probably dependent on its association with Max.

Repression of Cell Proliferation and Colony Formation

It has been shown that Mad1 and Mxi1 proteins repress cell proliferation and colony formation [Ayer et al., 1993; Zervos et al., 1993; Hurlin et al., 1995]. To confirm the ability of hMad4 to repress cell growth, we investigated the proliferation of HeLa and 293 cells infected with a bi-cistronic retrovirus coding for both hMad4 and GFP and then sorted by FACS to yield a 100% hMad4-expressing cell population. Western blot analysis of cell extracts from these infected cells is depicted in Figure 4A. hMad4 is detected only in hMad4-infected cells. In fact, no endogenous hMad4 is detected in empty-vector-infected cells. β-actin was used as a loading control. To test the ability of hMad4 to actively repress cell proliferation, 5×10^4 sorted hMad4-infected HeLa and 293 cells were plated on a 6-well plate. For 3 consecutive days, cells were harvested and counted on a hematocytometer

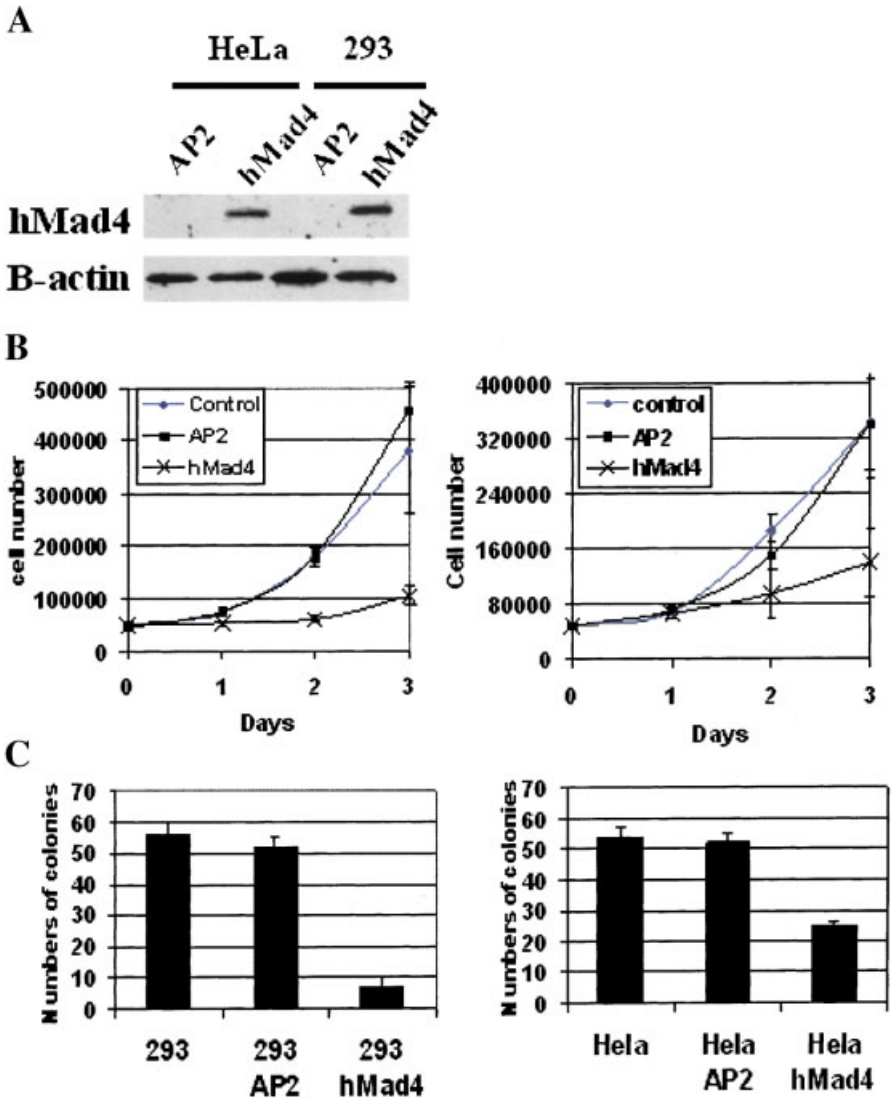

Fig. 4. Effect of hMad4 on cell proliferation and contact inhibition. **A**: Extracts from empty-vector- and AP2-hMad4-infected sorted cells were subjected to Western blot analysis using anti-hMad4 antibody. Blots were stripped and re-probed with β-actin as a loading control. **B**: Equal number of sorted cells was plated on day 0. Every day for 3 days, cell number was determined for non-infected (control), empty-vector (AP2)-, and AP2-hMad4-infected HeLa (**left**) and 293 (**right**) cells. The experiment was done in triplicate. **C**: Non-infected (control), empty-vector (AP2)-, and AP2-hMad4-infected cells were plated in soft agar. After 2 weeks, total number of colonies was counted from infected HeLa (**left**) and 293 (**right**) cells. Experiment was done in triplicate.

under a light microscope (Fig. 4B). Growth was repressed by about 4- and 2.5-fold in 293- and HeLa-hMad4 infected cells, respectively. This repression of cell proliferation was accompanied by an increase in contact inhibition in a soft agar colony assay (Fig. 4C). Total colony formation was almost totally (over 10-fold) repressed in 293 hMad4-infected cells, while effects were milder in HeLa hMad4-infected cells, colony formation being repressed by about 2.5-fold compared to both non-infected and empty-vector-infected cells.

hMad4 Induced a Complete Growth Arrest in Human Fibroblasts

The fact that hMad4 regulation in normal replicative senescent fibroblasts is altered, suggested that maybe hMad4 played a role in either establishing or maintaining the senescent phenotype. To test this, we infected young WI38 cells with hMad4 as well as a mutant hMad4 (hMad4L-P16), where a leucine (amino acid 16) was changed for a proline in the SID. This mutant is defective in transcriptional

repression as reported for mouse Mad1 and Mxi1 [Ayer et al., 1995; Schreiber-Agus et al., 1995] (data not shown). After infection, GFP-expressing cells were sorted and plated at equal densities. Cells were passaged every 4 days to ensure that confluency was not reached. After 48 days, the empty-vector-infected cells (AP2) reach a plateau, with features similar to replicative senescence such as flat morphology, inability to reach confluence, and s-β-galactosidase expression (not shown). In the case of hMad4-infected cells, following a small and very slow proliferative phase from day 1 to day 26 following replating, cells completely stopped dividing at which point they acquire the morphological features of replicative senescence such as flat and enlarged morphology. The mutated hMad4 gave a slight replicative advantage compare to the empty-vector-infected cells, where there was almost a 3-fold increase in total cell number. Moreover, while the empty-vector-infected cells division rate slowed down around 38 days to a complete stop at day 43, hMad4L-P16-infected cells were still replicating at day 38 until they reach an end at day 54 (Fig. 5A), where they acquire a senescent-like phenotype.

To test whether the proliferative arrest seen in hMad4-infected cells was replicative senescence, at day 30, we stained the infected cells for s-β-galactosidase expression since it's a marker for replicative senescence [Dimri et al., 1995]. hMad4-infected cells did express s-β-galactosidase expression while empty-vector- and hMad4L-P16-infected cells had a very low expression level (typical image in Fig. 6A). Over 300 cells were visualized for s-β-galactosidase expression and graphed in Figure 6B. While

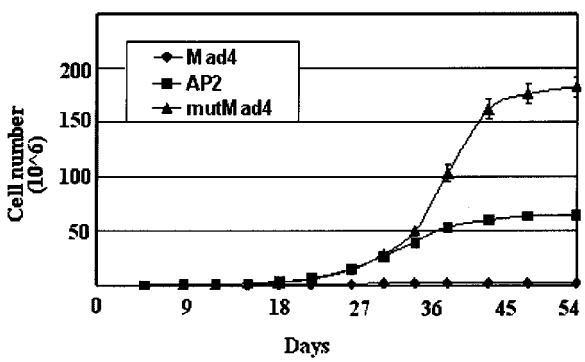

Fig. 5. Cell growth curve of infected cells. Infected WI38 cells were passed and counted with a hematocytometer where at least six fields were counted, every 4–5 days. Results are depicted in the graph and were done in triplicate.

both control- and mutant-infected cells had a very low expression level, hMad4-infected had a 4.5-fold increase in blue staining at day 30, suggesting that cells are entering replicative senescence. To further confirm that, indeed hMad4-infected cells were entering replicative senescence, we tested infected cells for Pai-1 expression, a protein upregulated in replicative senescence [Goldstein et al., 1994]. Only hMad4-infected cells had a high expression level of Pai-1 protein (Fig. 6C). Overall, these results suggest that overexpression of hMad4 in WI38 fibroblasts induces a replicative-like senescent phenotype.

DISCUSSION

We report here the isolation and characterization of a human Max-interacting protein, hMad4. Since hMad4 contains a basic helix-loop-helix-leucine-zipper (bHLHZip) structure, a high identity (90%) with the murine homologue mMad4 reported by Hurlin et al. [1995], and localizes to a region syntenic to mouse Mad4 because FGFR3, which is adjacent to mMad4 on chromosome 5, is adjacent to hMad4 on chromosome 4p16.3, hMad4 is likely the human counterpart of mouse Mad4. In light of the high degree of conservation of critical domain sequence information between human and murine Mad4, it is not surprising that hMad4 possesses similar properties and functions as murine Mad4 as a transcriptional repressor in human cells as demonstrated by Figure 3. Furthermore, the conservation of SID found in hMad4 (Fig. 1B) also strongly suggests that hMad4, similar to murine Mad4, may interact with the transcriptional co-repressor mSin3, bridging hMad4 with histone deacetylases.

We also demonstrate that hMad4 is ubiquitously expressed in many tissues, although some tissue like liver has very low level. So far no study has been done for tissue distributions of Mad4 in mouse. The only known observation shows that mouse Mad4 is expressed mainly in terminally differentiated cells during development. Moreover, its expression is often the last observed during developmental stage as compared with other Mad members. This finding actually suggest that it might be regulated by its sister genes' expression [Queva et al., 1998].

Expression of hMad4 leads to transcriptional repression as depicted in Figure 3. hMad4 seems to have the same potency as mouse Mad4 to repress c-Myc transcriptional activity

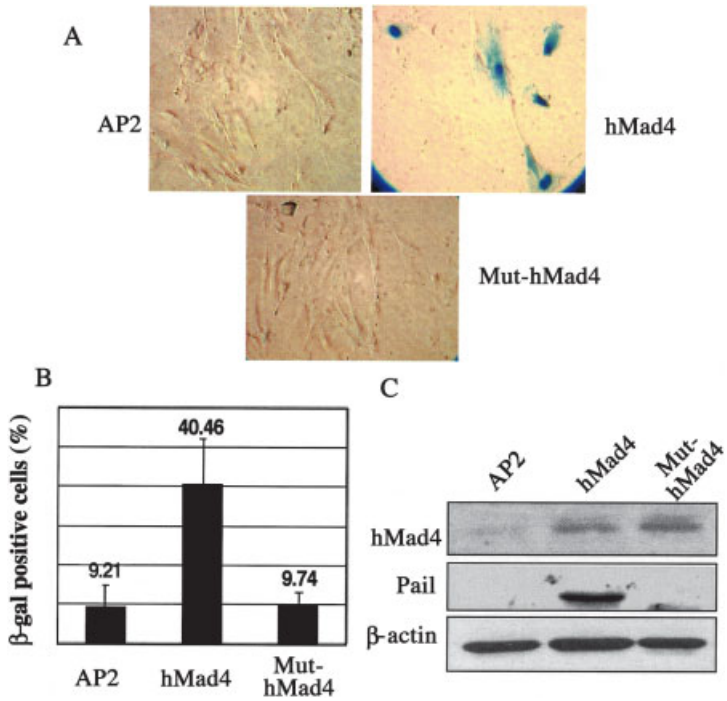

Fig. 6. Characterization of hMad4-infected cells. **A**: Pictures of empty-vector (AP2)-, hMad4-, and hMad4L-P16-infected cells. Cells were fixed and stained for s-β-galactosidase expression. Positive cells were counted in twenty different fields and results are shown in (**B**). **C**: Western blot of hMad4, Pai-1, and β-actin. Fifty micrograms of protein were run on 12% SDS–PAGE. Dilutions were 1:2,000 for hMad4 antibody, 1:1,000 for Pai-1, antibody, and 1:8,000 for β-actin.

under reporter assay since Hurlin et al. [1995] obtained a 5-fold decrease in CAT activity using a 3-fold excess of mouse Mad4 over c-Myc. In our case, hMad4 induce a 4-fold repression at equimolar ratio of c-Myc. Hence, the strong potency of hMad4 to repress transcription is accompanied by a strong ability to greatly reduce cell proliferation. While mouse Mad4's ability to prevent cell proliferation was not reported, Mad1 was less potent in slowing down proliferation in several cell lines, never reaching more than a 3-fold decrease in cell proliferation [Chen et al., 1995; Gehring et al., 2000]. In our case, repression reached 4.5-fold in 293 cells (Fig. 4B). Moreover, hMad4 transcriptional repression activity also impaired colony-forming potential of 293 and HeLa cells, reaching 10-fold in 293 cells. This inhibition was not due to the slower growth rate of these cells since total number of colonies were counted. In a conventional Ras + Myc transformation of rat embryo fibroblasts assay, mouse Mad4 repress colony production by 5-folds. Interestingly, in our case, hMad4 represses colony formation of cell line not transformed by c-Myc but by E6 and E7 papilloma virus protein and E1A in HeLa and 293 cells, respectively, reminiscent of results with Mad1, which inhibited colony formation by E6, E7, E1a, and mutated p53 [Cerni et al., 1995]. These results suggest that hMad4 could potentially repress transformation of highly heterogonous tumor cells and act as a very potent tumor suppressor.

It has been shown that rat fibroblasts null for c-Myc have an extended cell cycle doubling time of about 52 h compare to the 24 h of wild-type cells [Mateyak et al., 1997]. This lengthening in doubling time is due to both an increase in G1 and G2 phase times. These results were similar in mouse embryonic fibroblasts (MEFs), in which c-Myc was conditionally inactivated by the Cre-Lox system [de Alboran et al., 2001]. Most probably the net outcome of a complete inactivation of c-Myc is an increase in Mad members' functionality, therefore an increase transcriptional repression. Careful examination of hMad4-infected normal fibroblasts suggest that these cells are not instantly growth arrested but undergo an extremely slow replicative phase, in which the population doubled every 9–10 days. After 26 days, the cell population completely stopped dividing, entering a

replicative senescent-like state (Fig. 5), after only three population doublings following infection versus nine population doublings for the empty-vector-infected cells. This finding is intriguing because other protein like Ras, or reintroduction of wild-type p53 or p16 in deficient cells, instantaneously (4–6 days) induces a phenotype reminiscent of replicative senescence [Serrano et al., 1997; Sugrue et al., 1997; Uhrbom et al., 1997]. In fact, kinetics of the response to hMad4 resembles induction of replicative senescence by H_2O_2, histone deacetylase inhibitor, and topoisomerase inhibitors [Chen and Ames, 1994; Ogryzko et al., 1996; Michishita et al., 1998], which suggest some kind of stress response which causes lengthening of the cell cycle traverse and slowing of the cell cycle traverse. This stress, however, is unlikely mediated by introduction of the transgene since mutated hMad4 did not cause this phenotype. Therefore, this phenotype is most likely induced by the transcriptional repressor activity of hMad4. Nevertheless, the replicative senescent phenotype seen by the continuous presence of high hMad4 expression by the retroviral vector may be due to the gradual switching over of the heterodimeric complex from the c-Myc/Max to the hMad4/Max, until all the available endogenous Max molecules are exhaustively bound by the transgene protein product. This gradual shift may be the main reason explaining the long duration, i.e., 26 days and three population doublings later, the replicative senescent phenotype is achieved, in contrast to the induction seen in 3 days by Ras-overexpression, which may largely work through the MAP kinase signaling pathways. In all, our finding shows that replicative senescent phenotype can be obtained by a transcriptional repressor whose chief function is to compete with c-Myc for the same binding partner while exerting no transactivating action for the downstream gene activation for all the E-box containing genes.

ACKNOWLEDGMENTS

We thank Dr. J. Campisi for the human senescent fibroblast cDNA library, Dr. J. Galipeau for providing the Ap2 vector and packaging cell line, Dr. Abelnaby Khalyfa for the hMad4 antibody, Francis Hong for assistance in the preparation of figures, and Denis Bourbeau and Emmanuel Petroulakis for technical advices. The authors are also indebted to Mr. Alan N. Bloch for proofreading this manuscript.

REFERENCES

Amati B, Brooks MW, Levy N, Littlewood TD, Evan GI, Land H. 1993a. Oncogenic activity of the c-Myc protein requires dimerization with Max. Cell 72:233–245.

Amati B, Littlewood TD, Evan GI, Land H. 1993b. The c-Myc protein induces cell cycle progression and apoptosis through dimerization with Max. Embo J 12:5083–5087.

Ayer DE, Eisenman RN. 1993. A switch from Myc:Max to Mad:Max heterocomplexes accompanies monocyte/macrophage differentiation. Genes Dev 7:2110–2119.

Ayer DE, Kretzner L, Eisenman RN. 1993. Mad: A heterodimeric partner for Max that antagonizes Myc transcriptional activity. Cell 72:211–222.

Ayer DE, Lawrence QA, Eisenman RN. 1995. Mad-Max transcriptional repression is mediated by ternary complex formation with mammalian homologs of yeast repressor Sin3. Cell 80:767–776.

Baxendale S, MacDonald ME, Mott R, Francis F, Lin C, Kirby SF, James M, Zehetner G, Hummerich H, Valdes J, et al. 1993. A cosmid contig and high resolution restriction map of the 2 megabase region containing the Huntington's disease gene. Nat Genet 4:181–186.

Bello-Fernandez C, Packham G, Cleveland JL. 1993. The ornithine decarboxylase gene is a transcriptional target of c-Myc. Proc Natl Acad Sci USA 90:7804–7808.

Berberich S, Hyde-DeRuyscher N, Espenshade P, Cole M. 1992. Max encodes a sequence-specific DNA-binding protein and is not regulated by serum growth factors. Oncogene 7:775–779.

Blackwell TK, Kretzner L, Blackwood EM, Eisenman RN, Weintraub H. 1990. Sequence-specific DNA binding by the c-Myc protein. Science 250:1149–1151.

Blackwood EM, Eisenman RN. 1991. Max: A helix-loop-helix zipper protein that forms a sequence-specific DNA-binding complex with Myc. Science 251:1211–1217.

Blackwood EM, Luscher B, Eisenman RN. 1992. Myc and Max associate in vivo. Genes Dev 6:71–80.

Cerni C, Bousset K, Seelos C, Burkhardt H, Henriksson M, Luscher B. 1995. Differential effects by Mad and Max on transformation by cellular and viral oncoproteins. Oncogene 11:587–596.

Chen Q, Ames BN. 1994. Senescence-like growth arrest induced by hydrogen peroxide in human diploid fibroblast F65 cells. Proc Natl Acad Sci USA 91:4130–4134.

Chen J, Willingham T, Margraf LR, Schreiber-Agus N, DePinho RA, Nisen PD. 1995. Effects of the MYC oncogene antagonist, MAD, on proliferation, cell cycling, and the malignant phenotype of human brain tumour cells. Nat Med 1:638–643.

Coller HA, Grandori C, Tamayo P, Colbert T, Lander ES, Eisenman RN, Golub TR. 2000. Expression analysis with oligonucleotide microarrays reveals that MYC regulates genes involved in growth, cell cycle, signaling, and adhesion. Proc Natl Acad Sci USA 97:3260–3265.

Cultraro CM, Bino T, Segal S. 1997. Function of the c-Myc antagonist Mad1 during a molecular switch from proliferation to differentiation. Mol Cell Biol 17:2353–2359.

Dang CV. 1999. c-Myc target genes involved in cell growth, apoptosis, and metabolism. Mol Cell Biol 19:1–11.

de Alboran IM, O'Hagan RC, Gartner F, Malynn B, Davidson L, Rickert R, Rajewsky K, DePinho RA, Alt FW. 2001. Analysis of C-MYC function in normal cells via conditional gene-targeted mutation. Immunity 14: 45–55.

Dimri GP, Lee X, Basile G, Acosta M, Scott G, Roskelley C, Medrano EE, Linskens M, Rubelj I, Pereira-Smith O, et al. 1995. A biomarker that identifies senescent human cells in culture and in aging skin in vivo. Proc Natl Acad Sci USA 92:9363–9367.

Facchini LM, Penn LZ. 1998. The molecular role of Myc in growth and transformation: Recent discoveries lead to new insights. Faseb J 12:633–651.

Foley KP, McArthur GA, Queva C, Hurlin PJ, Soriano P, Eisenman RN. 1998. Targeted disruption of the MYC antagonist MAD1 inhibits cell cycle exit during granulocyte differentiation. Embo J 17:774–785.

Galipeau J, Li H, Paquin A, Sicilia F, Karpati G, Nalbantoglu J. 1999. Vesicular stomatitis virus G pseudotyped retrovector mediates effective in vivo suicide gene delivery in experimental brain cancer. Cancer Res 59: 2384–2394.

Gehring S, Rottmann S, Menkel AR, Mertsching J, Krippner-Heidenreich A, Luscher B. 2000. Inhibition of proliferation and apoptosis by the transcriptional repressor Mad1. Repression of Fas-induced caspase-8 activation. J Biol Chem 275:10413–10420.

Goldstein S, Moerman EJ, Fujii S, Sobel BE. 1994. Overexpression of plasminogen activator inhibitor type-1 in senescent fibroblasts from normal subjects and those with Werner syndrome. J Cell Physiol 161:571–579.

Guo QM, Malek RL, Kim S, Chiao C, He M, Ruffy M, Sanka K, Lee NH, Dang CV, Liu ET. 2000. Identification of c-myc responsive genes using rat cDNA microarray. Cancer Res 60:5922–5928.

Hann SR, Thompson CB, Eisenman RN. 1985. c-myc oncogene protein synthesis is independent of the cell cycle in human and avian cells. Nature 314:366–369.

Hassig CA, Fleischer TC, Billin AN, Schreiber SL, Ayer DE. 1997. Histone deacetylase activity is required for full transcriptional repression by mSin3A. Cell 89:341–347.

Hurlin PJ, Queva C, Koskinen PJ, Steingrimsson E, Ayer DE, Copeland NG, Jenkins NA, Eisenman RN. 1995. Mad3 and Mad4: Novel Max-interacting transcriptional repressors that suppress c-myc dependent transformation and are expressed during neural and epidermal differentiation. Embo J 14:5646–5659.

Kato GJ, Barrett J, Villa-Garcia M, Dang CV. 1990. An amino-terminal c-myc domain required for neoplastic transformation activates transcription. Mol Cell Biol 10:5914–5920.

Koskinen PJ, Ayer DE, Eisenman RN. 1995. Repression of Myc-Ras cotransformation by Mad is mediated by multiple protein–protein interactions. Cell Growth Differ 6:623–629.

Kozak M. 1987. An analysis of 5′-noncoding sequences from 699 vertebrate messenger RNAs. Nucleic Acids Res 15: 8125–8148.

Laherty CD, Yang WM, Sun JM, Davie JR, Seto E, Eisenman RN. 1997. Histone deacetylases associated with the mSin3 corepressor mediate mad transcriptional repression. Cell 89:349–356.

Lahoz EG, Xu L, Schreiber-Agus N, DePinho RA. 1994. Suppression of Myc, but not E1a, transformation activity by Max-associated proteins, Mad, and Mxi1. Proc Natl Acad Sci USA 91:5503–5507.

Luscher B, Eisenman RN. 1990. New light on Myc and Myb. Part I. Myc. Genes Dev 4:2025–2035.

Mateyak MK, Obaya AJ, Adachi S, Sedivy JM. 1997. Phenotypes of c-Myc-deficient rat fibroblasts isolated by targeted homologous recombination. Cell Growth Differ 8:1039–1048.

Michishita E, Nakabayashi K, Ogino H, Suzuki T, Fujii M, Ayusawa D. 1998. DNA topoisomerase inhibitors induce reversible senescence in normal human fibroblasts. Biochem Biophys Res Commun 253:667–671.

Nesbit CE, Tersak JM, Prochownik EV. 1999. MYC oncogenes and human neoplastic disease. Oncogene 18: 3004–3016.

Nesbit CE, Tersak JM, Grove LE, Drzal A, Choi H, Prochownik EV. 2000. Genetic dissection of c-myc apoptotic pathways. Oncogene 19:3200–3212.

O'Hagan RC, Schreiber-Agus N, Chen K, David G, Engelman JA, Schwab R, Alland L, Thomson C, Ronning DR, Sacchettini JC, Meltzer P, DePinho RA. 2000. Gene-target recognition among members of the myc superfamily and implications for oncogenesis. Nat Genet 24: 113–119.

Ogryzko VV, Hirai TH, Russanova VR, Barbie DA, Howard BH. 1996. Human fibroblast commitment to a senescence-like state in response to histone deacetylase inhibitors is cell cycle dependent. Mol Cell Biol 16:5210–5218.

Prendergast GC. 1999. Mechanisms of apoptosis by c-Myc. Oncogene 18:2967–2987.

Queva C, Hurlin PJ, Foley KP, Eisenman RN. 1998. Sequential expression of the MAD family of transcriptional repressors during differentiation and development. Oncogene 16:967–977.

Queva C, McArthur GA, Iritani BM, Eisenman RN. 2001. Targeted deletion of the S-phase-specific Myc antagonist Mad3 sensitizes neuronal and lymphoid cells to radiation-induced apoptosis. Mol Cell Biol 21: 703–712.

Rabbitts PH, Watson JV, Lamond A, Forster A, Stinson MA, Evan G, Fischer W, Atherton E, Sheppard R, Rabbitts TH. 1985. Metabolism of c-myc gene products: c-myc mRNA and protein expression in the cell cycle. Embo J 4:2009–2015.

Schreiber-Agus N, Chin L, Chen K, Torres R, Rao G, Guida P, Skoultchi AI, DePinho RA. 1995. An amino-terminal domain of Mxi1 mediates anti-Myc oncogenic activity and interacts with a homolog of the yeast transcriptional repressor SIN3. Cell 80:777–786.

Schreiber-Agus N, Meng Y, Hoang T, Hou H, Jr., Chen K, Greenberg R, Cordon-Cardo C, Lee HW, DePinho RA. 1998. Role of Mxi1 in ageing organ systems and the regulation of normal and neoplastic growth. Nature 393: 483–487.

Schuhmacher M, Kohlhuber F, Holzel M, Kaiser C, Burtscher H, Jarsch M, Bornkamm GW, Laux G, Polack A, Weidle UH, Eick D. 2001. The transcriptional program of a human B cell line in response to Myc. Nucleic Acids Res 29:397–406.

Serrano M, Lin AW, McCurrach ME, Beach D, Lowe SW. 1997. Oncogenic ras provokes premature cell senescence associated with accumulation of p53 and p16INK4a. Cell 88:593–602.

Sommer A, Bousset K, Kremmer E, Austen M, Luscher B. 1998. Identification and characterization of specific DNA-binding complexes containing members of the Myc/Max/Mad network of transcriptional regulators. J Biol Chem 273:6632–6642.

Sugrue MM, Shin DY, Lee SW, Aaronson SA. 1997. Wild-type p53 triggers a rapid senescence program in human tumor cells lacking functional p53. Proc Natl Acad Sci USA 94:9648–9653.

Uhrbom L, Nister M, Westermark B. 1997. Induction of senescence in human malignant glioma cells by p16INK4A. Oncogene 15:505–514.

Wang E. 1985a. Rapid disappearance of statin, a nonproliferating and senescent cell-specific protein, upon reentering the process of cell cycling. J Cell Biol 101: 1695–1701.

Wang E. 1985b. Disappearance of statin, a protein marker for non-proliferating and senescent cells, following serum-stimulated cell cycle entry. Exp Cell Res 167: 135–143.

Zervos AS, Gyuris J, Brent R. 1993. Mxi1, a protein that specifically interacts with Max to bind Myc-Max recognition sites. Cell 72:223–232.